Research paper

Overall buckling performance of high strength steel welded I-sections under combined axial compression and bending

Bin Huang[1], Wen-Fu Zhang[2]

Abstract: This paper presents a numerical investigation into the high strength steel (HSS) welded I-section overall buckling performance with respect to the major axis under combined axial compression and bending. The validation of FE models compared with the existing test data to verify the appropriateness of the element division and boundary condition was firstly conducted. In line with the FE arrangement verified, separate 890 numerical models, covering a broader range of eight steel grades (460 MPa, 500 MPa, 550 MPa, 620 MPa, 690 MPa, 800 MPa, 890 MPa and 960 MPa), different overall slenderness and various eccentricities were designated. Subsequently, the comparison of the resistance prediction codified design rules in EN1993-1-1, ANSI/AISC 360-10 and GB50017-2017 was preferentially operated, by the instrumentality of the normalized axial compression-bending moment curves. The results graphically revealed that, the provision given in ANSI/AISC 360-10 concerned in the present work was the most loose, whereas, the corresponding content set out in EN1993-1-1 and GB50017-2017 was relatively on the safe side. Taking account of the FE results, the conservative shortcomings of the considered rules in EN1993-1-1 and GB50017-2017 were further highlighted. Especially, the disparity of EN1993-1-1 and numerical results was higher to 27%, from the perspective of a definition given in the present work. In contrast, the provision in ANSI/AISC 360-10 yielded a relatively accurate prediction, on average. Based on the numerical program, an alternative formula for the HSS welded I-section beam-columns with a general expression form was sought, which intimately reflected the effect of overall slenderness.

Keywords: beam-columns, combined axial compression and bending, finite element analysis, high strength steel, overall buckling, welded I-section

---

[1]PhD., School of Civil Engineering and Architecture, Nanjing Institute of Technology, 211167 Nanjing, China, e-mail: 89690966@qq.com, ORCID: 0000-0002-8413-1280
[2]Prof., PhD., School of Civil Engineering and Architecture, Nanjing Institute of Technology, 211167 Nanjing, China, e-mail: zhangwf_2021@163.com, ORCID: 0000-0002-0848-4893

1. Introduction

New steel production technology has greatly improved the strength and process-ability of steel. Meanwhile, the weld metal materials and technology with sufficient strength, excellent toughness and ductility matching well with high strength steel (HSS, yield strength standard value $\geq$ 460 MPa) have been relatively mature, which are capable of fully meeting the processing and manufacturing requirements of components. These accumulated favorable factors make it possible for HSS to be employed in contemporary steel constructions. Material properties possess crucial impact on the member structural performance. Due to higher yield strength, the disparity of the mechanical behavior of the HSS components in contrast to the ones of conventional mill steel deserves to be paid adequate attention, especially on the buckling performance governing the ultimate load of compression members. In terms of our familiar buckling theories, it is well known that the buckling load of the ideal mechanical models is principally related to the cross-section geometry, member slenderness (or plate slenderness) and boundary conditions. Whilst, in the practical engineering, the buckling resistance of compression members is comprehensively restricted to the initial imperfections as well, which usually comprise residual stresses and geometric imperfections directly leading to the stiffness reduction and second order effect, respectively. According to the residual stress findings of HSS members [1, 2], there is no direct proportional relationship between the magnitude of residual stresses and the steel grades, which approximately indicates that the ratio of residual stresses to the yield strength of HSS is lower than the conventional mill steel. That means the effect resulted from residual stresses and second order effect is attenuated with HSS members [3]. As a consequence, it is questionable to directly mirror the codified design rules determined from the traditional mild steel study to the resistance predictions of HSS members.

To date, substantial achievements of buckling performance study on HSS welded members have been being gradually enriched, especially in the field of vertical load-bearing structural members. With regard to the columns, members subjected to exactly axial compression, the study result primarily involved high strength steel grades consist of Q460 (yield strength f_y = 460 MPa) [4], Q550 [5], Q690 [5], Q700 [6], Q960 [4], Q1100 [6] and Q1350 [7]. Meanwhile, regarding under the eccentric compression, i.e. subjected to axial compression and bending moment, the members combining the column function of transmitting axial forces with the beam function of transmitting moments, are usually defined as beam-columns, the investigation objective of the present study, which also attract attentions of practical engineers and academic researchers. In 2012, Li et al. [8] carried out an investigation of overall buckling factor around poor axis of Q460 welded H-section beam-columns. In 2014, Kim et al. [9] explored the effect of the plate-edge restraints and the width-thickness ratio on beam-columns of 800 MPa, and verified the applicability AISC $P–M$ interaction strength curve. In 2017, Ma et al. [10] published the test data of Q690 welded H-section beam-columns. In 2018, Gardner et al. [11] reported the test results of weld I-section beam-columns with average steel yield strength 330MPa and 390MPa. A literature review shows that: despite several concerns have been launched, most of the existed experimental investigation in parallel with numerical programs on the HSS welded

I-section beam-columns were mainly concentrated on one or two individual steel grades. In the present work, the investigation of HSS welded I-section beam-columns over a boarder range of steel grades including eight different steel grades (460 MPa, 500 MPa, 550 MPa, 620 MPa, 690 MPa, 800 MPa, 890 MPa and 960 MPa) was undertaken, with the aim of seeking economical but robust design resistance predictions for the HSS welded I-section beam-columns.

Aiming at the focus of the present study and following the summary of existing experimental study, a numerical modelling program developed in line with the FE arrangement validated against existing test results to generate the data pool was presented. Subsequently, the derived FE results were employed to investigate the overall buckling performance with respect to the major axis of HSS welded I-section beam-columns, and to assess the accuracy of the existing codified design rules given in the European code EN1993–1-1 [12], American specification ANSI/AISC 360-10 [13] and Chinese steel structure design standard GB50017-2017 [14]. Meanwhile, the shortcomings of the codified beam-column design provisions considered were identified, and new alternative formulas were then made to overcome the identified limits of the codified resistance prediction.

2. Finite element model and verification

2.1. Finite element model description

Geometric notation of I-section beam-columns buckled with respect to the major axis considered in the present work was labeled as I $H \times B \times t_f \times t_w$, with geometric dimension of section plates as shown in Fig. 1. Note that the test specimens buckled with respect to the poor axis just only adopted in the FE model verification were differentially labeled as H $H \times B \times t_f \times t_w$.
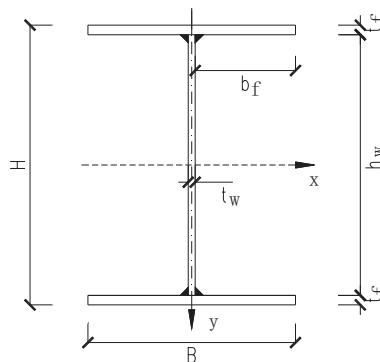

Fig. 1. Geometric notation for the I-section

The FE software ANSYS (Manuel 15.0) was adopted to execute numerical simulation. The nonlinear analyze capability of the software accounting for geometric and material

nonlinearity was turned on to derive the failure behavior and the ultimate load. Shell element Shell181 was used to discrete the steel welded I-section column geometric models and record the local deformation of beam-columns. Shell181 is capable of specifying unequal thicknesses, various material patterns, distinctive material directions and different integral point number for each layer of the element. Reasonable element sizes are favorable to enable the balance of computational accuracy and efficiency. Regarding the FE models considered, 22 elements were set along the flanges, and the corresponding element division number along the web and the axis of the member were determined according to the ratio $22h_w/B$ and $22L_{eff}/B$, (L_{eff} was the length of the numerical specimens) respectively, which ensured the element size to be essentially square. The overall buckling Euler critical load of ideal column model of FE models compared against the analytical solution are plotted in the Fig. 2, which was graphically evident the feasibility of the element size arrangement. Regarding the boundary conditions, the beam-column specimens were modelled with simple supports at the top and bottom ends.
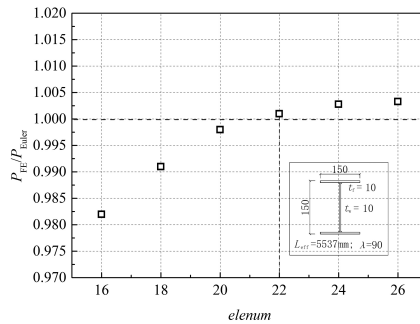

Fig. 2. Overall buckling critical load ratio of FE to analytical solution against
the flange element division quantity

The command "CERIG" was utilized to couple the end profile nodes to the centroid node of the top or bottom end sections, respectively, which allowed the end cross-sections to rotate freely about the consistent buckling axis and the top one to translate longitudinally. At the same time, lateral supports outside the bending moment plane were arranged to prevent the presumable buckling with respect to the I-section poor axis as shown in Fig. 3.

Owing to the randomness of material mechanical property, parameters of the constitutive relationship were assumed to be nominal ones according to the national standard [14]
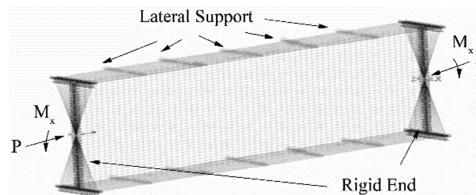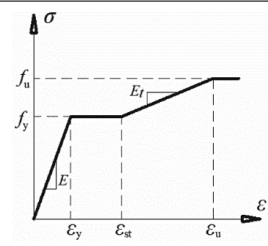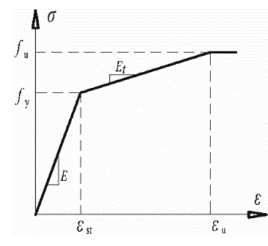

Fig. 3. Typical finite element model

as listed in Table 1, including elastic modulus E, yield strength f_y and tensile ultimate strength f_u.

Table 1. Parameters for constitutive model of HSS

Grade	E (MPa)	f_y (MPa)	f_u (MPa)	E_{st} (%)	ε_u (%)	Material constitutive relation
Q460	2.06×10^5	460	550	2.00	14.0	
Q500	2.06×10^5	500	610	f_y/E	10.0	
Q550	2.06×10^5	550	670	f_y/E	9.0	
Q620	2.06×10^5	620	710	f_y/E	9.0	
Q690	2.06×10^5	690	770	f_y/E	8.0	
Q800	2.06×10^5	800	840	f_y/E	7.0	
Q890	2.06×10^5	890	940	f_y/E	6.0	
Q960	2.06×10^5	960	980	f_y/E	5.5	

Quadruple-linear isotropic hardening material model was adopted to describe the strain-stress relationship of Q460; the trilinear isotropic hardening material model was applied for other steel grades, which have been put into numerical simulation practice of HSS columns [2]. For the considered initial imperfections, longitudinal residual stresses within cross-sections incorporated at the five integration points on the thickness were assumed to be constant along the thickness direction, the pattern of which was according to the findings in [4], derived from Q460 and Q960 columns using cutting strip method, as shown in Fig. 4a and 4b.
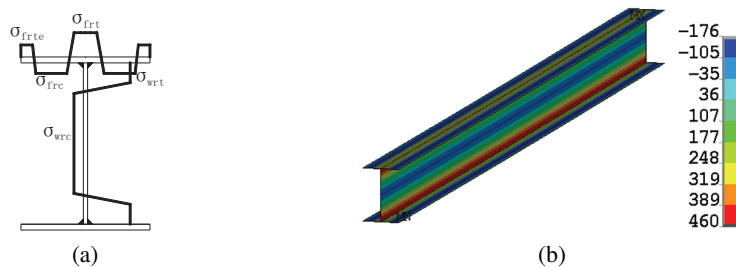

Fig. 4. Residual stress pattern: (a) Residual stresses; (b) Magnitude of the residual stresses incorporated into the Q460 beam-columns

Geometric imperfection naturally exists in practical compression members. In the present work, the first order flexural bending buckling mode taken as the geometric imperfection configuration of the column FE models, was employed to update the node coordinate prior to the static analysis, in conjunction with the amplitude of $L_{\text{eff}}/1000$, using the command "UPGEOM" provided in ANSYS.

2.2. Verification of FE models

Practical test programs have been carried out to investigate the HSS beam-columns buckling performance as mentioned earlier. At present, most of the overall buckling performance test studies were focused on the buckling behavior with respective to the poor axis. Detailed information of a total of 26 existing test specimens are listed in Table 2, including

Table 2. Compared of FEM and experiment specimens

Specimen	L_{eff} (mm)	Bending axis	e (mm)	$N_{\text{Exp.}}$ (kN)	$N_{\text{Exp.}}/N_{\text{FEM}}$	f_y (MPa)
I $161.1 \times 161.2 \times 13.06 \times 8.58$ (Gardner, 2018)	500	Major	70.2	1157.7	1.089	330
I $161.3 \times 160.7 \times 12 \times 8$	500	Major	75.1	1183.3	1.099	390
H $161.0 \times 161.4 \times 12.99 \times 8.57$	500	Minor	44.8	943.6	0.976	330
H $161.2 \times 160.8 \times 12.2 \times 8.3$	500	Minor	44.6	1138.8	1.023	390
I $310 \times 220 \times 15 \times 15$ (D.K. Kim, 2014)	900	Major	0.0	9042	0.942	760
I $310 \times 220 \times 15 \times 15$	900	Major	30	7084	0.995	760
I $310 \times 220 \times 15 \times 15$	900	Major	120	4672	0.994	760
I $310 \times 220 \times 15 \times 15$	900	Major	275	2864	1.015	760
H $140.0 \times 119.6 \times 9.90 \times 5.83$ (T.Y. Ma et al., 2017)	1992	Minor	100	328	1.079	756
H $141.2 \times 119.8 \times 9.91 \times 5.85$	2790	Minor	100	250	1.055	756
H $170.0 \times 149.3 \times 9.90 \times 5.81$	1993	Minor	100	527	1.021	756
H $170.0 \times 149.7 \times 9.92 \times 5.85$	2790	Minor	100	418	0.981	756
H $231.8 \times 201.5 \times 15.98 \times 9.92$	1993	Minor	100	1698	1.039	766
H $231.7 \times 200.7 \times 15.97 \times 9.95$	2792	Minor	100	1376	1.036	766
H $284.2 \times 250.1 \times 15.97 \times 9.92$	1991	Minor	100	2662	1.013	766
H $282.0 \times 249.9 \times 15.93 \times 9.93$	2790	Minor	100	2276	1.015	766
Mean					1.023	
Standard deviation					4.12%	

I-section and H-section, load eccentricity e, effective length L_{eff}, yield strength of steel f_y and ultimate applied load. The numerical replication of existing test specimens listed in Table 2 were performed to examine the approach of element division and boundary condition arrangement, where the material characteristics, boundary conditions, geometric imperfections and residual stresses were all followed in line with the source literatures [9–11]. For the test without explicit definition of the initial imperfection measurements, the test numerical simulation adopted the residual stress pattern "Ban" [2] aforementioned in Section 2.1. And the amplitude $L_{\text{eff}}/1000$ combined with the shape from overall buckling eigen-mode was taken as the overall imperfection as given in Section 2.1. Taken together, the average value of the ratio between the FE results and the test data was 1.035 and the standard deviation was 4.12%. Moreover, the load-end rotation (θ) curves of specimen A2 and B2 in [11], respectively obtained from tests and FE models were compared in Fig. 5. In general, the FE arrangement was feasible and reliable.
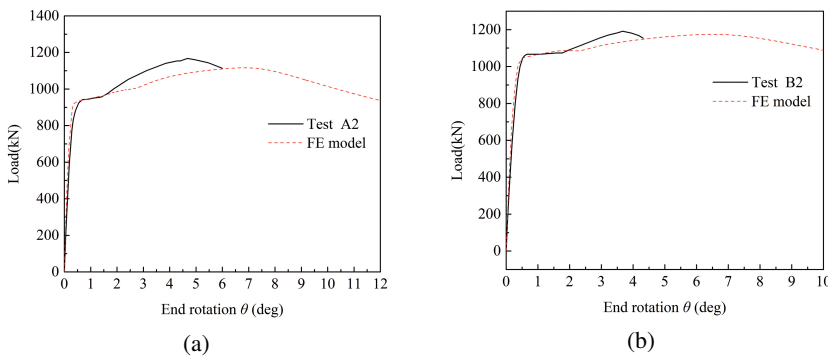

Fig. 5. Comparison of test and FE model load-end rotation (θ) curves: (a) A2 in [11]; (b) B2 in [11]

3. Interaction formula of beam-columns

At present, the most widely used method for describing buckling performance is essentially on the basis of the strength interactive formula. According to the edge fiber yield criterion, considering the second order effect of axial compression, the overall buckling behavior of beam-columns can be expressed as Eq. (3.1)

$$(3.1) \qquad \frac{P_u}{P_y} + \frac{M_u + P_u e_0}{M_y(1 - P_u/P_E)} = 1$$

where P_u and M_u are the applied loads of beam-columns; e_0 comprehensively reflected the effect of initial imperfections comprising geometric imperfection and residual stresses; $1/(1 - P_u/P_E)$ is the moment amplification factor considering second-order effect resulted from axial compression; $P_E = \pi^2 EI/L_{\text{eff}}^2$; $P_y = Af_y$; $M_y = W_e f_y$; W_e is the elastic section modulus. IF the plastic development γ_x of cross section was taken into account, Eq. (3.1)

was expressed as Eq. (3.2)

$$(3.2) \qquad \frac{P_u}{\varphi A f_y} + \frac{M_u}{\gamma_x W_e f_y \left(1 - \varphi P_u / P_E\right)} = 1$$

Despite the general concept of the beam-column overall buckling description given in Eq. (3.1) and Eq. (3.2), the disparity of the codified resistance predictions in accordance with Eurocode3 [12], ANSI/AISC 360-10 [13], and GB50017-2017 [14] is non-negligible, which was identified in this section. Firstly, the dissimilar expressions of the design rules according to various standard codes explicitly expressed in below sections were all transformed into a unified form expressed with M_d/M_{pl} and N_d/N_{pl}. N_d and M_d were the applied axial compression and bending moment, respectively. N_{pl} was equal to the area of the cross-sections multiplied by yield strength, and M_{pl} was the product of plastic section modulus and yield strength. Furthermore, the N_d/N_{pl} and M_d/M_{pl} could be regarded as the dimensionless axial compression N_d and bending moment M_d, which were normalized by N_{pl} and M_{pl}, respectively. In line with the considered different design provisions, given the value of N_d, the magnitude of M_d can be deduced, the interactive curves of which can be further derived. For example, knowing N_d, the M_d can be derived according to the provision in EN1993-1-1 expressed as Eq. (3.3). Then the dependence relation of N_d/N_{pl} and M_d/M_{pl} can be established. Imitating of the approach, the interactive formulas of M_d/M_{pl} and N_d/N_{pl} corresponding to ANSI/AISC360-10 [13] and GB50017-2017 [14] were also achieved, as plotted in Fig. 6.
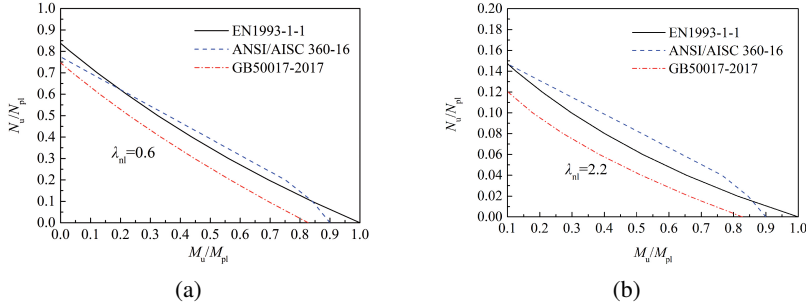

Fig. 6. Comparison of I-beam-columns provision of codes in this study (a) $\lambda_{nl} = 0.6$; (b) $\lambda_{nl} = 2.2$

It can be seen that, by comparison, provisions given in GB50017-2017 and EN1993-1-1 were conservative; whereas, the rules of ANSI/AISC360-10 is relative loose. The disparity of the considered standards were highlighted by the increasing slenderness λ_{nl}, observed from the contrast between Fig. 6a and 6b.

3.1. FE models for interaction formula study

Using the FE simulation approach examined, a total of separate 890 HSS beam-column FE models, covering a broader range of eight steel grades, member slenderness and eccentricity were established to explore the overall buckling resistance prediction and assess

the accuracy of the existing codified design rules, as shown in Table 3. Because of the study focus on the overall buckling, the geometric characteristics of FE models were designated to be belong to class 1 and class 2 according to EN1993-1-1 [12], which was set to avoid the interference of plate local buckling failure. Five dimensionless slenderness ratios $\lambda_{nl} = (\lambda/\pi)\sqrt{f_y/E}$ (the slenderness λ was a ratio of effective length L_{eff} to radius of gyration of cross-section i) and six eccentricity ratio $\varepsilon = e/(W_e/A)$ (e was load eccentricity; A was area of cross-section) attributes were assigned to four cross-section.

Table 3. Parameters of FE models

Parameters	Value
Steel strength f_y (MPa)	460, 500, 550, 620, 690, 800, 890, 960
λ_l	0.6, 1.0, 1.4, 1.8, 2.2
ε	0.4, 0.8, 1.2, 1.6, 3.0, 6.0
Cross-section	I $150 \times 150 \times 10 \times 10$, I $140 \times 120 \times 10 \times 6$ I $232 \times 200 \times 16 \times 10$, I $350 \times 230 \times 16 \times 12$
Initial geometric imperfection	Amplitude $l_{eff}/1000$ & Shape of first-order overall buckling eigenmode
Residual stress pattern	"Ban" [4]

3.2. EN1993-1-1

In EN1993-1-1 [12], the yield strength of structure steel is enhanced to 690MPa. The axial compression and bending moment interactive formula for the overall buckling of beam-columns is expressed as

$$(3.3) \qquad \frac{N_{Ed}}{\chi_x N_{RK}/\gamma_{M1}} + \frac{M_{x,Ed}}{\chi_{LT} M_{x,RK}/\gamma_{M1}} \leq 1$$

where N_{Ed}, $M_{x,Ed}$ are the design values of the compression force and the moment about the major axis along the member, respectively, χ_x is the reduction factor due to lateral buckling, χ_{LT} is the reduction factor due to lateral torsional buckling form.

Table 4 present the result by substituting the FE results into of the Eq. (3.3). It can be found the average values of each steel grade of Eq. (3.3) were all higher than 1.0 and up to 1.52 corresponding to 960 MPa, which was roughly decrease due to lower λ_{nl} and steel grades. The overall average regardless of various slenderness and steel grades of Eq. (3.3) based on the FE data was up to 1.27, which reflected the unduly conservatism of the direct application of EN1993-1-1 on high strength steel beam-columns. Figure 7 reports the $M_d/M_{pl} - N_d/N_{pl}$ curves of the FE models compared against codified design provisions. Except individual points lying below the codified curves, corresponding to the rather high slenderness, the FE data was primarily higher than the codified design rules. Meanwhile, the FE result scattered trend was decreased resulted from higher steel grades, which stemmed

principally from attenuated effects of residual stresses and geometric imperfections. The overly conservatism was largely attributed to the higher level of $N_{Ed}/(\chi_x N_{RK}/\gamma_{M1})$ in Eq. (3.3) resulted from unduly smaller χ_x. On the basis of existing experimental findings in [2, 4, 15], the curve a in Eurocode 3 was proposed to be incorporated in Eq. (3.3) for the resistance prediction of beam-columns of steel grade higher than 550.
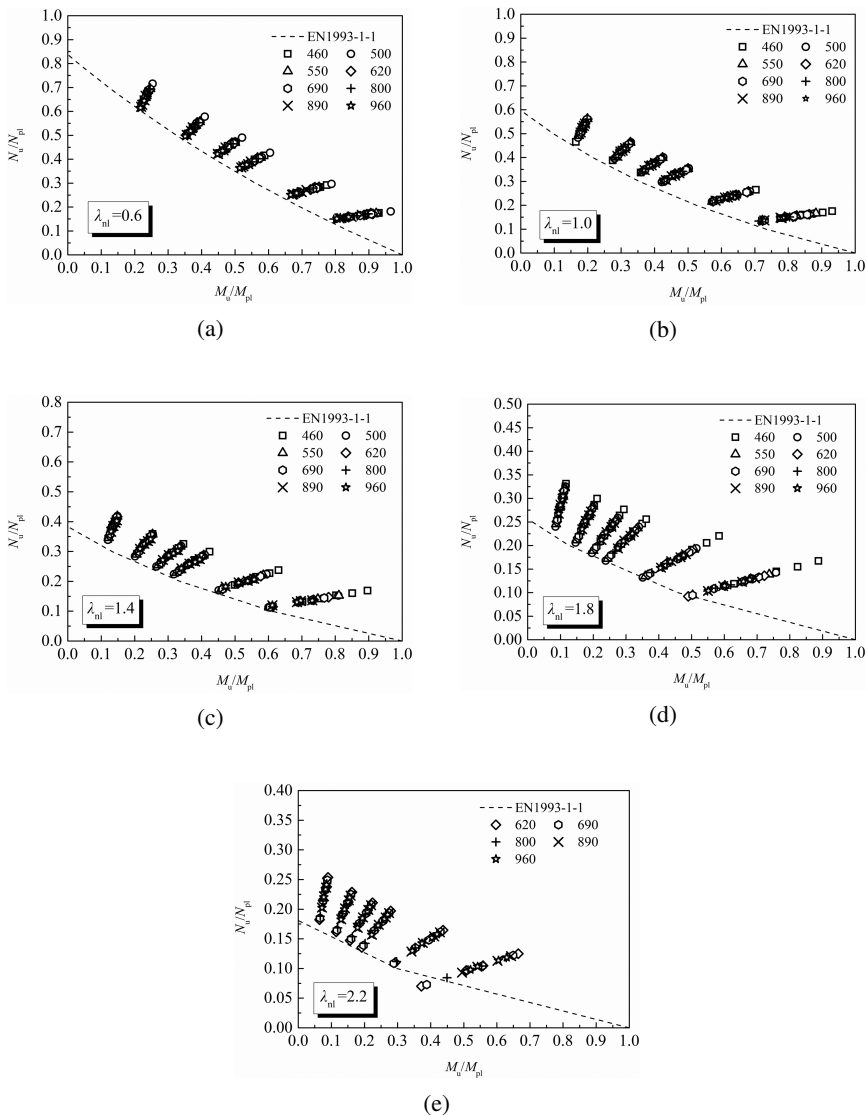

Fig. 7. Normalized compression and minor axes bending relationships of FE models and design results according to EN 1993-1-1: (a) $\lambda_{nl} = 0.6$; (b) $\lambda_{nl} = 1.0$; (c) $\lambda_{nl} = 1.4$; (d) $\lambda_{nl} = 1.8$; (e) $\lambda_{nl} = 2.2$

Table 4. The result of design rules in EN1993-1-1 based on the FE results

Steel grade	$Sum_{EC3} = \dfrac{N_{Ed}}{\chi N_{RK}/\gamma_{M1}} + \dfrac{M_{x,Ed}}{\chi_{LT} M_{x,RK}/\gamma_{M1}}$								
	Q460	Q500	Q550	Q620	Q690	Q800	Q890	Q960	Average
$\lambda_{nl} = 0.6$	1.133	1.162	1.143	1.138	1.137	1.127	1.075	1.056	1.121
$\lambda_{nl} = 1.0$	1.226	1.215	1.218	1.217	1.219	1.209	1.186	1.178	1.209
$\lambda_{nl} = 1.4$	1.336	1.254	1.257	1.257	1.256	1.251	1.249	1.245	1.263
$\lambda_{nl} = 1.8$	1.517	1.325	1.325	1.322	1.316	1.313	1.347	1.337	1.350
$\lambda_{nl} = 2.2$	1.520	1.425	1.411	1.377	1.36	1.364	1.406	1.404	1.408

3.3. ANSI/AISC 360-10

The yield strength of hot rolled section steel of ANSI/AISC 360-10 is up to 690MPa. The interactive factors for beam-column provisions given in ANSI/AISC360-10 are expressed as

$$\text{(3.4)} \qquad \frac{P_d}{P_c} + \frac{8}{9}\frac{M_{dx}}{M_{cx}} \leq 1.0; \quad \frac{P_d}{P_c} \geq 0.2$$
$$\frac{P_d}{2P_c} + \frac{M_{dx}}{M_{cx}} \leq 1.0; \quad \frac{P_d}{P_c} < 0.2$$

where $P_c = 0.9P_n$, $M_{cx} = 0.9M_n$, P_d is design axial load, M_{dx} was the design moment, P_n is the axial buckling resistance, $M_n = W_p f_y$, W_P is the plastic modulus of cross section in class 1 and class 2.

The interactive relationship of M_d/M_{pl} and N_d/N_{pl} derived from FE model results together with codified design provisions are described in Fig. 8. The average values of each steel grade of Eq. (3.4) by substituting N_d, M_d of FE result were slightly higher than 1.0 as shown in Fig. 8, on average, which reflected good applicability of ANSI/AISC360-10 for HSS I-section beam-columns.

3.4. GB50017-2017

Steel grade Q460 has been added to new Chinese steel structure design standard GB50017-2017. The interactive formula for the resistance prediction of beam-columns buckling with respect to the major axis of the I-section is expressed as

$$\text{(3.5)} \qquad \frac{N_d}{\varphi_x A f} + \frac{M_{dx}}{\gamma_x W_{ex}\left(1 - 0.8N_d/N'_{Ex}\right)f} \leq 1$$

where f was material design strength, equal to $f_y/1.111$; λ_x is overall slenderness for flexural buckling about the major axis; φ_x is overall buckling factor; $N'_{Ex} = \pi^2 EA/(1.1\lambda_x^2)$; γ_x is plasticity adaptation factor for bending about the major axis, which is taken as 1.05 for I-section beam-columns.
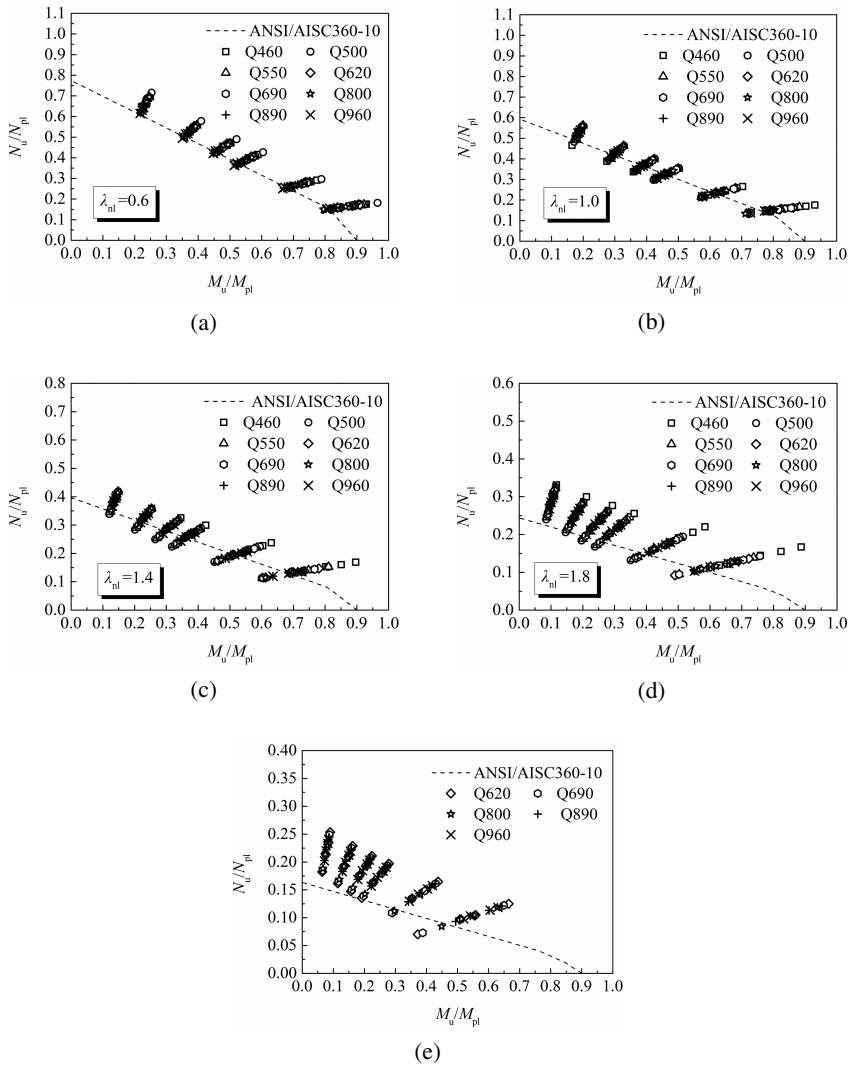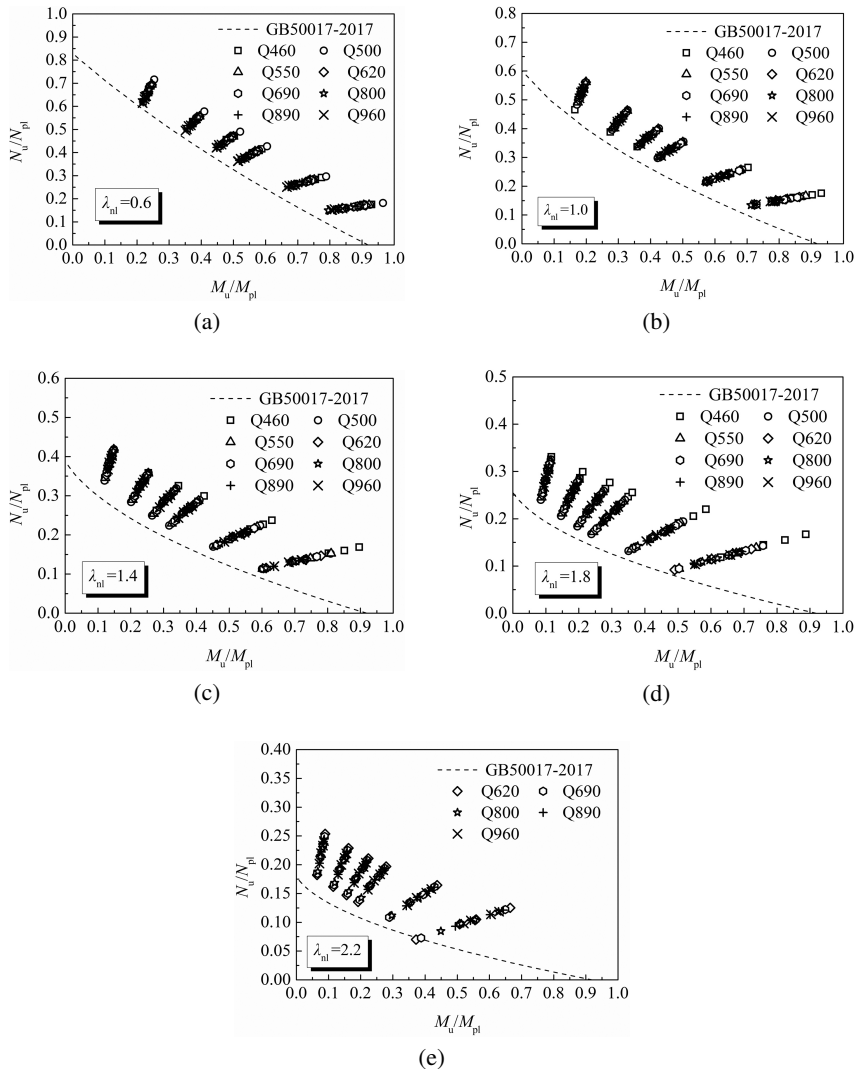
Fig. 8. Normalized compression and minor axes bending relationships of FE models and design results according to ANSI/AISC360-10: (a) $\lambda_{nl} = 0.6$; (b) $\lambda_{nl} = 1.0$; (c) $\lambda_{nl} = 1.4$; (d) $\lambda_{nl} = 1.8$; (e) $\lambda_{nl} = 2.2$

The normalized compression and major axis bending relationships of FE models together with design results are presented in Fig. 9. The average values of each steel grade of Eq. (3.5) by substituting N_d, M_d of FE results were all pronouncedly greater than 1.0 as shown in Fig. 9, which were enhanced in dependence of higher slenderness. As found in Section 3.2, the overall buckling factor curve for HSS according to GB50017-2017 was unduly conservative, which was verified in the test data [4, 15].

Fig. 9. Normalized compression and minor axes bending relationships of FE models and design results according to GB50017-2017: (a) $\lambda_{nl} = 0.6$; (b) $\lambda_{nl} = 1.0$; (c) $\lambda_{nl} = 1.4$; (d) $\lambda_{nl} = 1.8$; (e) $\lambda_{nl} = 2.2$

3.5. Development of interactive formula of beam-columns

From the discussion in Section 3.1–3.4, it was found that the form of the interactive formula was intimately dependent on the overall slenderness. A more general form of interactive formula for the HSS welded I-section beam-column overall buckling with respect to the major axis was established and expressed as Eq. (3.6). The form parameters ξ_P and

ξ_M of Eq. (3.6) were further determined based on the FE results of various λ_{nl}, as shown in Fig. 10a–10e.

$$(3.6) \qquad \left(\frac{P_u}{\varphi A f_y}\right)^{\xi_P} + \left(\frac{M_u}{\gamma_x W_e f_y (1 - \varphi P / P_E)}\right)^{\xi_M} = 1$$

$$(3.7) \qquad \xi_P = 2.027 - 1.595\lambda_{nl} + 0.779\lambda_{nl}^2 - 0.156\lambda_{nl}^3$$

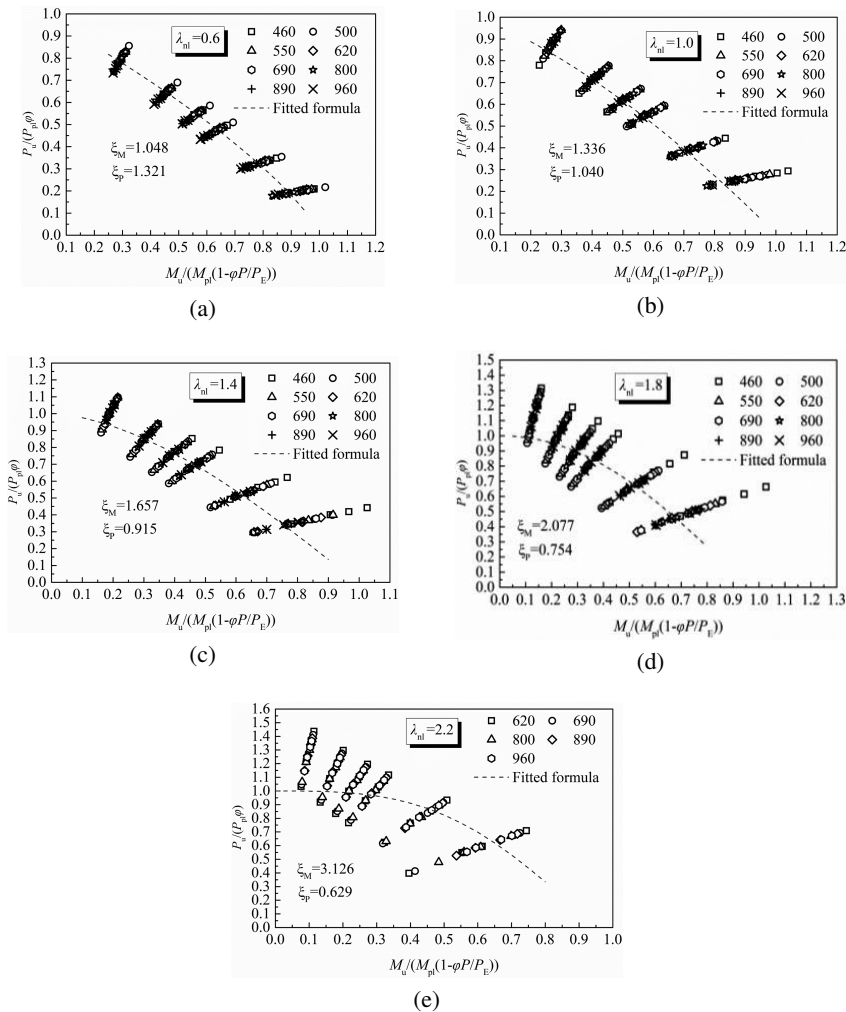$$(3.8) \qquad \xi_M = -0.214 + 3.332\lambda_{nl} - 2.530\lambda_{nl}^2 + 0.775\lambda_{nl}^3$$

Fig. 10. ξ_P and ξ_M fitted with FE results: (a) $\lambda_{nl} = 0.6$; (b) $\lambda_{nl} = 1.0$; (c) $\lambda_{nl} = 1.4$; (d) $\lambda_{nl} = 1.8$; (e) $\lambda_{nl} = 2.2$

The relationship of ξ_P, ξ_M and λ_{nl} were quantitative described as Eq. (3.7) and Eq. (3.8) by regression on the basis of FE data, as shown in Fig. 11. The result by substituting the FE result into the proposed resistance prediction approach Eq. (3.8) was defined as Eq. (3.9) to identify its applicability. Figure 12 reports the result of $Sum_{proposed}$ under various member slenderness λ_{nl} and different steel grades. It can be found that the value of $Sum_{proposed}$ graphically slightly higher than 1.0, with an average in the range from 1.01 to 1.14, which revealed more accurate and less scattered strength prediction of the proposed approach.

$$(3.9) \qquad Sum_{proposed} = \left(\frac{P_u}{\varphi A f_y} \right)^{\xi_P} + \left(\frac{M_u}{\gamma_x W_e f_y (1 - \varphi P / P_E)} \right)^{\xi_M}$$
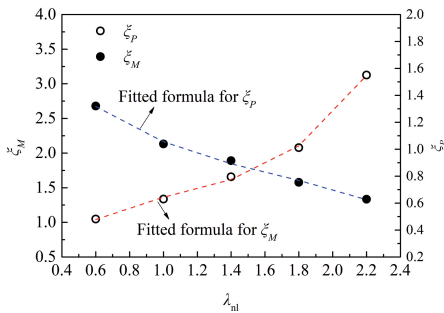

Fig. 11. Relationship of
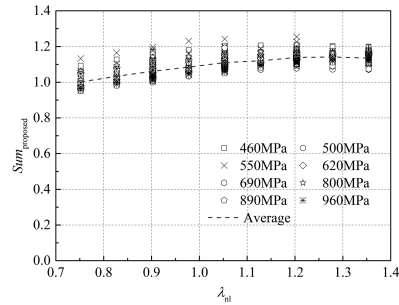ξ_P, ξ_M and λ_{nl}

Fig. 12. The accuracy description of the
proposed resistance prediction

4. Conclusions

In the present study, the performance of welded I-section beam-columns of eight steel grades (Q460, Q500, Q550, Q620, Q690, Q800, Q890, Q960) buckled with respect to the major axis were investigated based on the separate 890 FE models, the development approach of which was verified against existing test data. Subsequently, the accuracy of beam-column codified design rules given in Eurocode3, ANSI/AISC 360-10 and GB50017-2017 was examined by the instrumentality of the comparison with the FE results. An alternative formula for resistance prediction of HSS welded I-section beam-columns buckled with respective to major axis was developed on the basis of the numerical program. Overall, following conclusions were made:

– Regarding the comparison of the codified design rules given in various standards considered in the present work, under the identically overall slenderness and constant bending moment action, the corresponding provisions set out by ANSI/AISC 360-10 presented the most high axial compression loading-bearing, while the rules given in GB50017-2017 and Eurocode3 provided a lower axial compression prediction.

– Taking account of the FE result, the resistance prediction provisions in Eurocode3, as well as those in GB50017-2017 similarly present an unduly conservatism, the shortcoming of which was further exposed under the cases of higher levels of steel grades and overall slenderness.

– Overall, the codified design rules for the beam-columns set out by ANSI/AISC 360-10 yields a relatively appropriate prediction accuracy, observed form the comparison of the numerical program against the considered standard rules.

– Given the results generated by the numerical program, a development formula was proposed, intimately reflecting the effect of overall slenderness of beam-columns, which was evident to yield a more accurate and less scattered resistance prediction.

Acknowledgements

References

[1] K.J.R. Rasmussen, G.J. Hancock, "Tests of high strength steel columns", *Journal of Constructional Steel Research*, 1995, vol. 34, no. 1, pp. 27–52, DOI: 10.1016/0143-974X(95)97296-A.

[2] H.Y. Ban, G. Shi, "Overall buckling behavior and design of high-strength steel welded section columns", *Journal of Constructional Steel Research*, 2018, vol. 143, pp. 180–195, DOI: 10.1016/j.jcsr.2017.12.026.

[3] G.A. Marzahn, M. Hamme, W. Prehn, "International Association for Bridge and Structural Engineering", *Traffic engineering & technology for national defence*, 1932.

[4] H.Y. Ban, "Research on the overall buckling behavior and design method of high strength steel columns under axial compression", D.Sc. thesis, Tsinghua University, Beijing, 2012.

[5] G. Shi, X. Zhu, H.Y. Ban, "Material properties and partial factors for resistance of high-strength steels in China", *Journal of Constructional Steel Research*, 2016, vol. 121, pp. 65–79, DOI: 10.1016/j.jcsr.2016.01.012.

[6] M. Clarin, "High Strength Steel: Local Buckling and Residual Stresses", M.A. thesis, Luleĺ University of Technology, Sweden, 2004.

[7] X.L. Zhao, "Section capacity of very high strength (VHS) circular tubes under compression', *Thin Wall Structures*, 2000, vol. 37, no. 3, pp. 223–40, DOI: 10.1016/S0263-8231(00)00017-3.

[8] G.Q. Li, X.L. Yan, S.W. Chen, "Experimental study on bearing capacity of welded H-section columns using Q460 high strength steel under bending and axial compression", *Journal of Building Structures*, 2012, vol. 33, no. 12, pp. 31–37.

[9] D.K. Kim, C.H. Lee, K.H. Han, J.H. Kim, S.E. Lee, H.B. Sim, "Strength and residual stress evaluation of stub columns fabricated from 800 MPa high-strength steel", *Journal of Constructional Steel Research*, 2014, vol. 102, pp. 111–120, DOI: 10.1016/j.jcsr.2014.07.007.

[10] T.Y. Ma, Y.F. Hu, X. Liu, G.Q. Li, K.F. Chung, "Experimental investigation into high strength Q690 steel welded H-sections under combined compression and bending", *Journal of Constructional Steel Research*, 2017, vol. 138, pp. 449–462, DOI: 10.1016/j.jcsr.2017.06.008.

[11] X. Yun, L. Gardner, N. Boissonnade, "Ultimate capacity of I-sections under combined loading – Part 1: Experiments and FE model validation", *Journal of Constructional Steel Research*, 2018, vol. 147, pp. 408–421, DOI: 10.1016/j.jcsr.2018.04.016.

[12] European Committee for Standardization (CEN), "Eurocode 3-Design of Steel Structures – Part 1–1: General Rules and Rules for Buildings", Brussels, 2005.

[13] AISC, "ANSI/AISC 360-10, Speci?cation for structural steel buildings", Chicago, 2010.

[14] Ministry of housing and urban rural development of the people's Republic of China, "Code for Design of Steel Structures", China Architecture & Building Press, Beijing, 2018.

[15] T.J. Li, S.W. Liu, G.Q. Li, S.L. Chan, Y.B. Wang, "Behavior of Q690 high strength steel columns: Part 1: Experimental investigation", *Journal of Constructional Steel Research*, 2016, vol. 123, pp. 18–30, DOI: 10.1016/j.jcsr.2016.03.026.